



## Research Report

# The distribution and nature of responses to broadband sounds associated with pitch in the macaque auditory cortex



Yukiko Kikuchi <sup>a,b,\*</sup>, Sukhbinder Kumar <sup>a,c</sup>, Simon Baumann <sup>a</sup>, Tobias Overath <sup>d</sup>, Phillip E. Gander <sup>e</sup>, William Sedley <sup>a</sup>, Roy D. Patterson <sup>f</sup>, Christopher I. Petkov <sup>a,b,1</sup> and Timothy D. Griffiths <sup>a,c,e,\*</sup>

<sup>a</sup> Institute of Neuroscience, Newcastle University Medical School, Newcastle upon Tyne, UK

<sup>b</sup> Centre for Behaviour and Evolution, Newcastle University, Newcastle upon Tyne, UK

<sup>c</sup> Wellcome Trust Centre for Neuroimaging, University College London, UK

<sup>d</sup> Department of Psychology and Neuroscience, Duke University, Durham, NC, USA

<sup>e</sup> Department of Neurosurgery, University of Iowa, Iowa City, USA

<sup>f</sup> Department of Physiology, Development and Neuroscience, University of Cambridge, Cambridge, UK

## ARTICLE INFO

## Article history:

Received 3 August 2018

Reviewed Jan 15, 2019

Revised 25 March 2019

Accepted 10 July 2019

Action editor Carmen Cavada

Published online 18 July 2019

## Keywords:

Local field potentials

Single neuron

Rhesus

Auditory cortex

Pitch

## ABSTRACT

The organisation of pitch-perception mechanisms in the primate cortex is controversial, in that divergent results have been obtained, ranging from a single circumscribed ‘pitch centre’ to systems widely distributed across auditory cortex. Possible reasons for such discrepancies include different species, recording techniques, pitch stimuli, sampling of auditory fields, and the neural metrics recorded. In the present study, we sought to bridge some of these divisions by examining activity related to pitch in both neurons and neuronal ensembles within the auditory cortex of the rhesus macaque, a primate species with similar pitch perception and auditory cortical organisation to humans. We demonstrate similar responses, in primary and non-primary auditory cortex, to two different types of broadband pitch above the macaque lower limit in both neurons and local field potential (LFP) gamma oscillations. The majority of broadband pitch responses in neurons and LFP sites did not show equivalent tuning for sine tones.

© 2019 Published by Elsevier Ltd.

\* Corresponding author. Institute of Neuroscience, Newcastle University Medical School, Newcastle upon Tyne, UK.

E-mail addresses: [yukiko.kikuchi@newcastle.ac.uk](mailto:yukiko.kikuchi@newcastle.ac.uk) (Y. Kikuchi), [tim.griffiths@newcastle.ac.uk](mailto:tim.griffiths@newcastle.ac.uk) (T.D. Griffiths).

<sup>1</sup> Co-senior authors.

<https://doi.org/10.1016/j.cortex.2019.07.005>

0010-9452/© 2019 Published by Elsevier Ltd.

## 1. Introduction

This work uses the macaque as a neural model for human pitch perception and assesses single neuron- and ensemble-level bases for pitch perception. The communication sounds of humans and other mammals have components with relatively broad spectra. This is because the source of excitation is a temporally regular stream of glottal pulses produced by the larynx, and the spectrum of such a sound consists, essentially, of harmonics of the pulse rate with varying amplitudes (Ives & Patterson, 2008). The pulse rate is the fundamental (F0) of the harmonic series and it is the pitch we hear when presented with a communication sound (e.g., vocalization). In this study, we assess the basis of pitch perception in the macaque at the single-unit and neuronal-ensemble level using temporally regular sounds with broad spectra, and compare it with what is known about the corresponding pitch mechanisms in the human, marmoset and ferret. The macaque is a good model for human pitch perception both in terms of behaviour (Ghazanfar et al., 2007; Joly et al., 2014) and in terms of the fundamental anatomical and physiological organisation of auditory cortex (Baumann, Petkov, & Griffiths, 2013; Hackett, 2011). The assessment of neural spiking activity can be compared with pitch correlates observed in other mammals such as the marmoset (Bendor & Wang, 2005) and the ferret (Walker, Bizley, King, & Schnupp, 2011). Oscillations in local field potentials (LFP) arising from neural ensembles have been shown to occur in association with pitch perception in humans and other mammals (Bizley, Walker, Nodal, King, & Schnupp, 2013; Griffiths et al., 2010), and they can be assessed in the macaque alongside spiking activity. LFP oscillations also correlate with blood flow change (Logothetis, Pauls, Augath, Trinath, & Oeltermann, 2001; Mukamel et al., 2005) which is used as an indirect measure of neural activity related to pitch in human studies (see (Griffiths & Hall, 2012) for a review).

Any neural mechanism related specifically to the processing of pitch, as opposed to lower level sensory cues, should only appear when those sensory cues are associated with the perception of pitch. The lower limit of pitch is about 30 Hz in both humans (Krumbholz, Patterson, Seither-Preisler, Lammertmann, & Lütkenhöner, 2003; Pressnitzer, Patterson, & Krumbholz, 2001) and macaques (Joly et al., 2014); in humans, temporally regular sounds with lower repetition rates produce the perception of flutter, which is a salient acoustic feature, but not a sensation of pitch. Our first criterion for evidence of pitch processing, therefore, is that the mechanism should only be active for repetition rates above the lower limit of pitch. Accordingly, we sought activity that fades away as the repetition rate of the stimulus proceeds down through the lower limit of pitch. A second criterion for any pitch mechanism is that similar activity should be observed when the same pitch is perceived, irrespective of the specific acoustic structure of the associated stimulus. We assessed this using two different broadband stimuli known to produce broadband pitch: regular interval noise (RIN: (Patterson, Handel, Yost, & Datta, 1996)) and harmonic complex tones (HCTs).

Previous studies (e.g., (Bendor & Wang, 2005)) have imposed another criterion for a pitch response: there should be similar responses to the pitches of HCTs and sine tones. We did not impose this criterion in the present work, as there could well be separate mechanisms for the processing of HCTs and sine tones. We have, however, explored the relationship between putative pitch responses defined by the criteria above and the frequency tuning associated with sine tones, in order to assess the effect of this criterion. Previous work based on pitch responses in single neurons that included this criterion in the definition demonstrated a cluster of pitch selective responses in an area of cortex that overlapped anterolateral A1 and adjacent belt regions (Bendor & Wang, 2005). Previous human work based on the recording of LFPs (Griffiths et al., 2010) demonstrates responses to broadband stimuli associated with pitch in high-frequency gamma oscillations that were maximal in auditory core regions, but also more widely distributed across belt homologues. Indirect studies of ensemble responses associated with pitch based on human functional imaging (Hall & Plack, 2009; Norman-Haignere, Kanwisher, & McDermott, 2013; Patterson, Uppenkamp, Johnsrude, & Griffiths, 2002; Penagos, Melcher, & Oxenham, 2004) have demonstrated peak responses to pitch correlates in likely homologues of belt cortex (Baumann et al., 2013; Hackett, 2011). Thus, depending on species, pitch criteria, and recording modality, putative pitch responses have been seen that are either circumscribed or widely distributed, and can be maximal in core, belt or overlap regions/homologues (see (Griffiths et al., 2010) for discussion).

The present study aimed to bridge some of the divides between these studies with disparate methodologies and findings, by reporting direct recordings of single neuron and ensemble responses in multiple auditory areas of the awake macaque. We assessed the spiking activity of single neurons and local field potentials from groups of neurons in areas of macaque cortex including A1 and adjacent belt areas. We applied minimum criteria related to the lower limit of pitch and similar responses to different broadband sounds with the same pitch to both types of response in order to demonstrate pitch-selective responses, and to allow their mapping within auditory cortex. We also examined common responses to the pitch of broadband sounds and sine tones in order to highlight the proportion of putative pitch processing responses meeting that criterion. The data demonstrate the existence of putative pitch responses in the form of spiking activity in single neurons and high-frequency oscillatory gamma responses that represent activity in neuronal ensembles. Some clustering of these responses is demonstrated in the anterolateral border of A1 overlapping with adjacent belt regions, but both types of response occur more widely, across other parts of auditory cortex. The majority of such broadband pitch-related responses in single units and LFP sites did not show similar responses to sine tones.

## 2. Results

A total of 149 local field potentials (LFP) (Monkey A:  $n = 83$ ; Monkey B:  $n = 66$ ) and 210 single-unit activity (SUA) recordings

(Monkey A:  $n = 120$ ; Monkey B:  $n = 90$ ) with significant auditory responses (see Material and Methods) were recorded either separately or, more often, simultaneously using two to three independently driven electrodes from tonotopically organized regions of auditory cortex in two macaques. The animals listened passively to auditory stimuli which consisted of a .5-sec burst of noise, a .9-sec pitch-evoking stimulus (RIN or HCT), and another .9-sec burst of noise. There was a simultaneous visual fixation task (see Fig. 1 and Materials and Methods). The criteria for a *pitch response* for LFP and SUA are as follows: 1) both RIN and HCT have to elicit a significant auditory response (2SD above the baseline activity 500 ms prior to sound onset) at the same pitch value, 2) the pitch value eliciting the maximum response, defined as the best rate (BR), has to be the same and above the macaque lower limit of pitch ( $\sim 30$  Hz) (Joly et al., 2014), and 3) the response magnitude elicited by a pitch-evoking stimulus has to be greater than that evoked by a control sound (continuous broadband noise).

Out of 149 LFP and 210 SUA recordings from the auditory cortices of two macaques, 17% of LFP ( $n = 26$ ) and 13% of single-units ( $n = 28$ ) met the criteria for a putative pitch response. Single-unit activity normally showed a robust onset response to the first noise burst and decayed over time during the burst. Since the power of the stimulus does not change when the noise is replaced by a pitch-evoking stimulus with the same bandwidth, the change in neuronal response at this juncture was associated with the temporal structure of the sound. Furthermore, because perceptual features of regular temporal structure not relating to pitch are present both above and below its lower limit, neural responses occurring at this

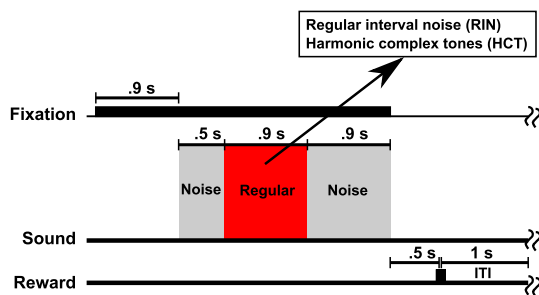


**Fig. 1 – Behavioural task.** The animal was trained to perform a fixation task and initiated a trial by fixating a spot for 900 ms, triggering sound presentation. While fixating, the animal passively listened to stimuli comprising a .5 sec broadband noise burst preceding .9 sec of pitch-evoking regular stimulus (RIN or HCT) followed by another noise burst for .9 sec. The animal was required to fixate on the spot until the sound turned off for 2.3 sec to receive a reward (juice drop,  $\sim 2$  ml), which occurred approximately  $\sim 500$  ms after the offset of sound presentation. The RIN was created from a random phase broadband noise using 16 iterations of a delay-and-add algorithm (Yost, 1996) with a delay of 1/16, 1/32, 1/64, 1/128, 1/256, and 1/512, and that result in pitch values at 16, 32, 64, 128, 256, and 512 Hz, for each of which three exemplars were created. Random-phase harmonic tones were also created with fundamental frequencies,  $F_0$ , of 16, 32, 64, 128, 256, and 512 Hz.

transition only to stimuli with  $f_0$  above the lower limit most likely relate specifically to the processing of pitch itself.

Fig. 2 shows examples of single neurons showing a pitch-related response. At the presentation of the first noise, these neurons showed a significant onset response that decayed over time. A significant rate specific response was observed in response to both RIN and HCT at the transition from the first noise to the regular stimulus. Unit A in Fig. 2A is an example of a pitch-related unit showing increased firing rates in response to RIN and HCT during the presentation of pitch-evoking stimuli with maximum firing rates at a best rate (BR) of 512 Hz (RIN:  $23.4 \pm 6.5$  spikes/s; HCT:  $14.2 \pm 5.1$  spikes/s, mean  $\pm$  SD, Fig. 2B). Unit B shows an increase in firing rates during the presentation of both RIN and HCT at a different rate (BR = 64 Hz) compared to the response to the preceding noise (RIN:  $18.3 \pm 6.1$  spikes/s, HCT:  $12.7 \pm 5.1$  spikes/s). Although these pitch-related units have different BRs, they exhibit similar tuning functions in response to RIN and HCT (Unit A:  $\rho = .66$ ,  $p = .18$ , Unit B:  $\rho = .94$ ,  $p < .02$ , Spearman correlation, Fig. 2B). These units were recorded from low-frequency anterolateral auditory cortex (Fig. 2C). Tuning curves for all single-units that showed responses associated with pitch are shown in Figure S1.

We examined the relationship between SUA and LFPs recorded from the same sites. Among the 28 SUA and 26 LFP pitch sensitive sites, the recorded SUA and LFP were both pitch-related responses in seven sites (SUA: 25%; LFP: 27%) and they shared the same BRs in three out of seven sites (43%). Example SUA and LFP responses, recorded simultaneously from a single site are shown in Fig. 3. The single neuron recording shows a robust increase in firing rates in response to both HCT and RIN with the maximum response magnitude at 128 Hz (RIN:  $158.1 \pm 51.0$  spikes/s, HCT:  $131.6 \pm 46.6$  spikes/s). Fig. 3A (top panels) shows the time-frequency representation of LFP responses to RIN and HCT. The simultaneously recorded LFP shows sustained auditory oscillatory activity particularly in high-gamma frequency range ( $>80$  Hz) which is also maximum for a stimulus rate of 128 Hz at the transition from the first noise to pitch-evoking stimuli compared to the response to noise as a baseline. The SUA and LFP responses to multiple pitch values of this example are shown in Figure S2. The LFP high-gamma power ( $>80$  Hz) and SUA showed similar tuning functions in response to both stimulus types at the level of single-unit and neuronal ensembles (SUA:  $\rho = 1.0$ ; LFP:  $\rho = .9$ ,  $p < .02$ , Spearman correlation, Fig. 3B).

Fig. 4 shows another example of a significant pitch-related LFP response with significant induced responses compared to power increase during the preceding noise presentation ( $p < .01$ , bootstrap significance level) with a spectrum peak in the high gamma range ( $\sim 100$  Hz). Measurement of the inter-trial-phase coherence (ITC) in the high-gamma range demonstrates that the response is truly induced, with no phase-locked component ( $p < .01$ , bootstrap, Fig. 4A). Transient phase-locked low frequency evoked potentials to sound onset and transitions are also demonstrated by this analysis. Turning curves and the location for this unit are shown in Fig. 4B and C ( $\rho = .9$ ,  $p = .08$ , Spearman correlation). Tuning curves for all LFPs that showed pitch-related responses are shown in Figure S3. All the correlation values are also mapped on the STP in Figure S4.

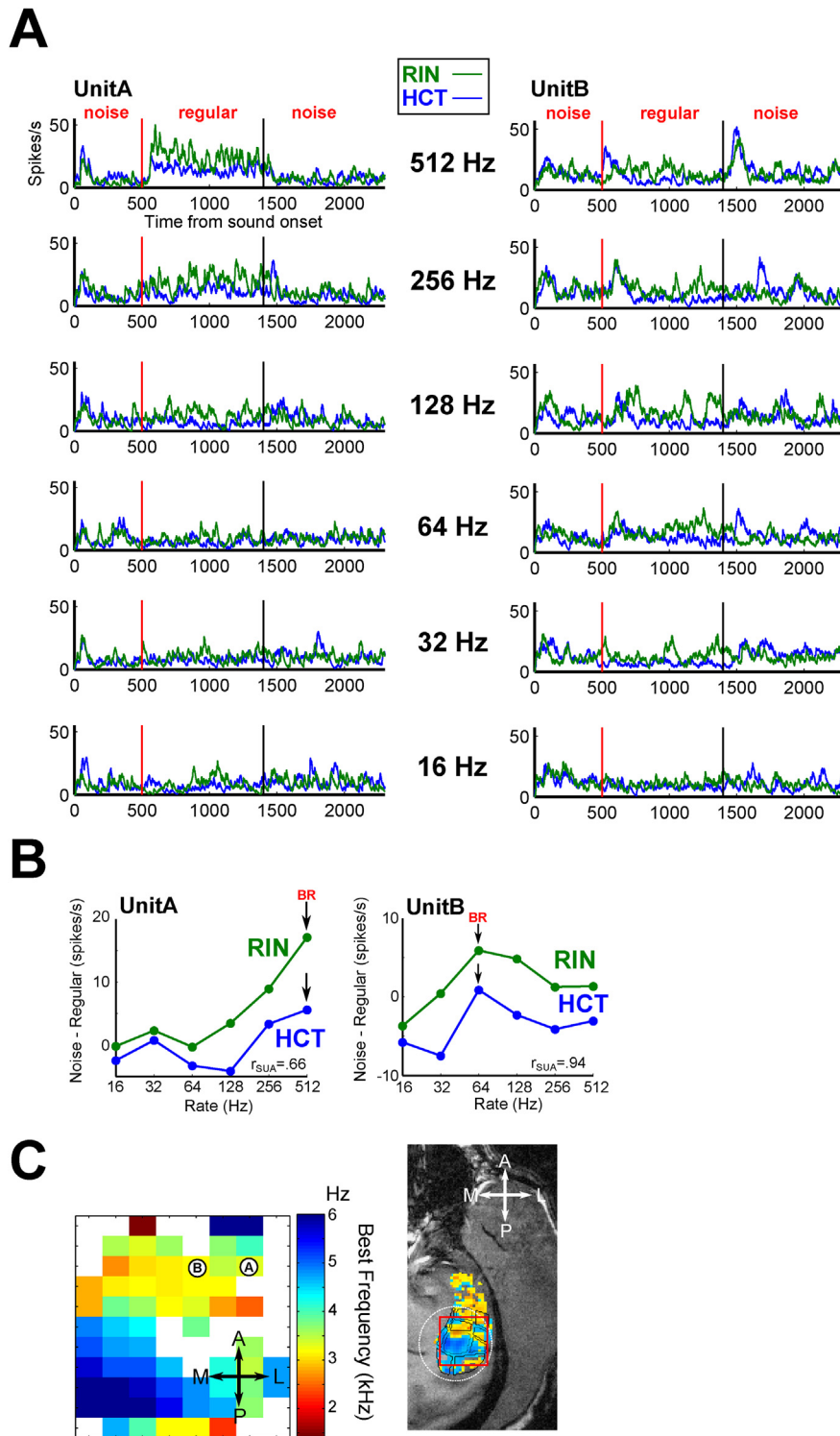


**Fig. 2** – Examples of single neurons showing pitch responses to a RIN and a HCT. **(A)** Averaged PSTHs of the responses of Unit A and Unit B aligned to sound onset in response to RINs (green lines) and HCTs (blue lines) at different rates (16–512 Hz). Unit B also shows the responses after the offset of pitch-evoking stimuli. The vertical red line marks the onset of a regular stimulus and the vertical black line marks the offset of a regular stimulus. **(B)** Tuning curves for Unit A and B, shown in **(A)**. The tuning curves were constructed from the increase in firing rate during regular stimulus presentation (501–1400 ms) minus the mean firing rate in response to the preceding noise (1–500 ms). The tuning curve in response to RIN is shown by the green curve (i.e., RIN - Noise); the tuning curve in response to HCT is shown by the blue curve (i.e., HCT - Noise). The arrows denote the neurons' best rates (BR) with maximum response-magnitudes in the tuning curves. **(C)** Locations of the single neurons for Unit A (a circle plot with 'A') and Unit B (a circle plot with 'B') showing pitch SUA responses in the left panel. The background colour map depicts the tonotopic map based on the averaged best frequencies

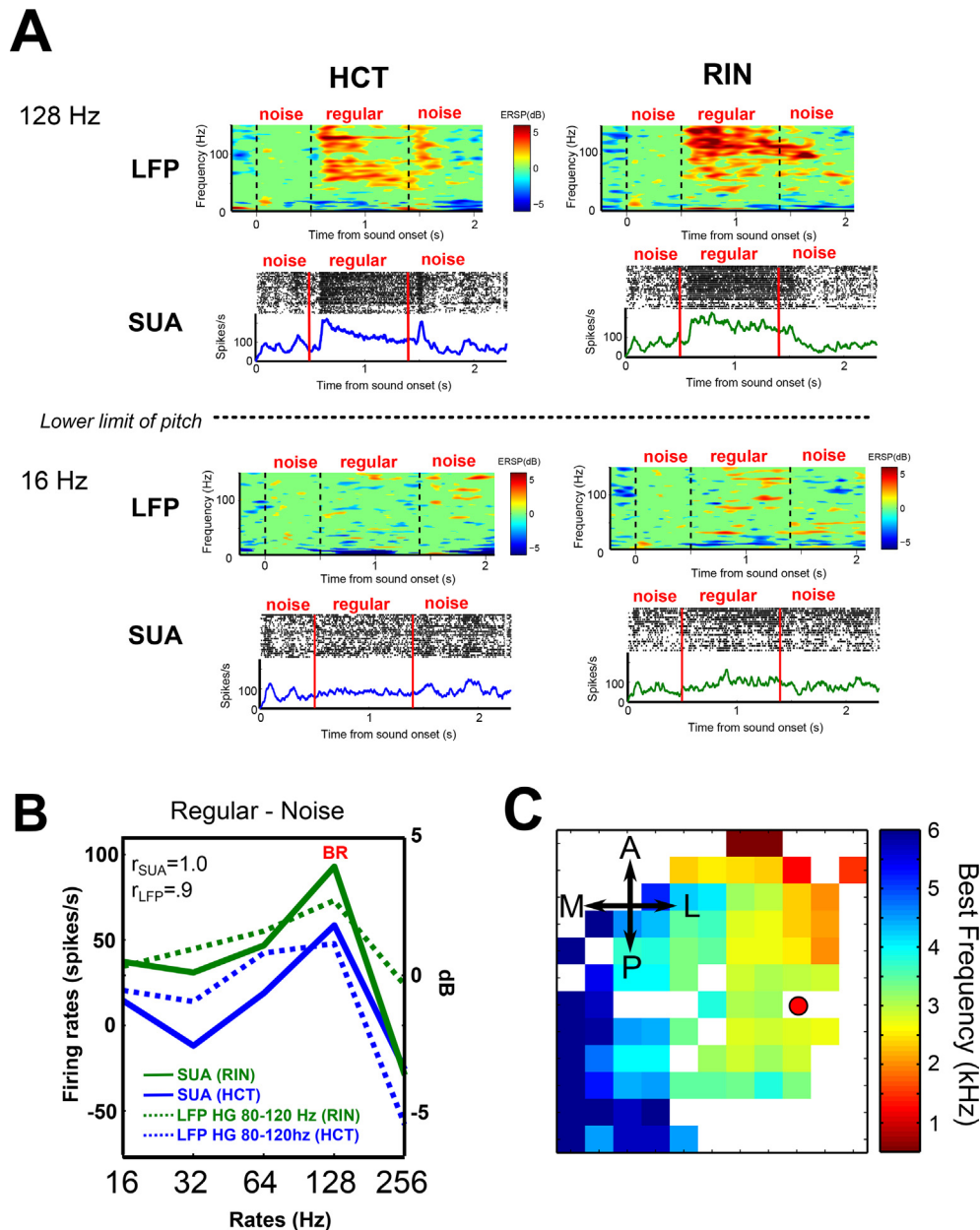


**Fig. 3** – Comparison of neuronal tuning to rates below and above the lower limit of pitch in response to RIN and HCT at the level of single-unit activity (SUA) and LFP. **(A)** Examples of LFP and SUA responses to RIN and HCT. The upper panels show the event-related spectral perturbation (ERSP) time-frequency decomposition of LFPs across trials. The colour scale represents power change normalised by the power change at each frequency using the entire period of first noise presentation (0–500 ms prior to onset of a regular stimulus), expressed in decibels (dB). The lower panels show spike rasters (upper graph) and PSTHs (lower graph) aligned to sound onset of SUA recorded from the same electrode that recorded the LFP shown in the upper panel. **(B)** Tuning curves in response to RIN (green) and HCT (blue) at multiple repetition rates shown in **(A)**. The solid lines show the tuning curve of SUA in response to RIN (green) and HCT (blue) and the dotted lines show the tuning curve of the LFP in response to RIN (green) and HCT (blue). **(C)** The red circle shows the location of the recording site for the unit exhibiting the pitch responses shown in **(A)** and **(B)**. The background colour map depicts the tonotopic map based on the averaged BFs of single-unit activity of the right STP of Monkey B (1-mm grid spacing).

(BF) of auditory neurons (>3SD from baseline firing rates) recorded in each cell of the right supratemporal plane (STP) of Monkey B. The right panel shows the location of recording chamber (dotted white circle) where the MRI-based tonotopic map was superimposed on the right supratemporal plane (STP) of Monkey A and the location of recording site (red square) shown on the left panel.

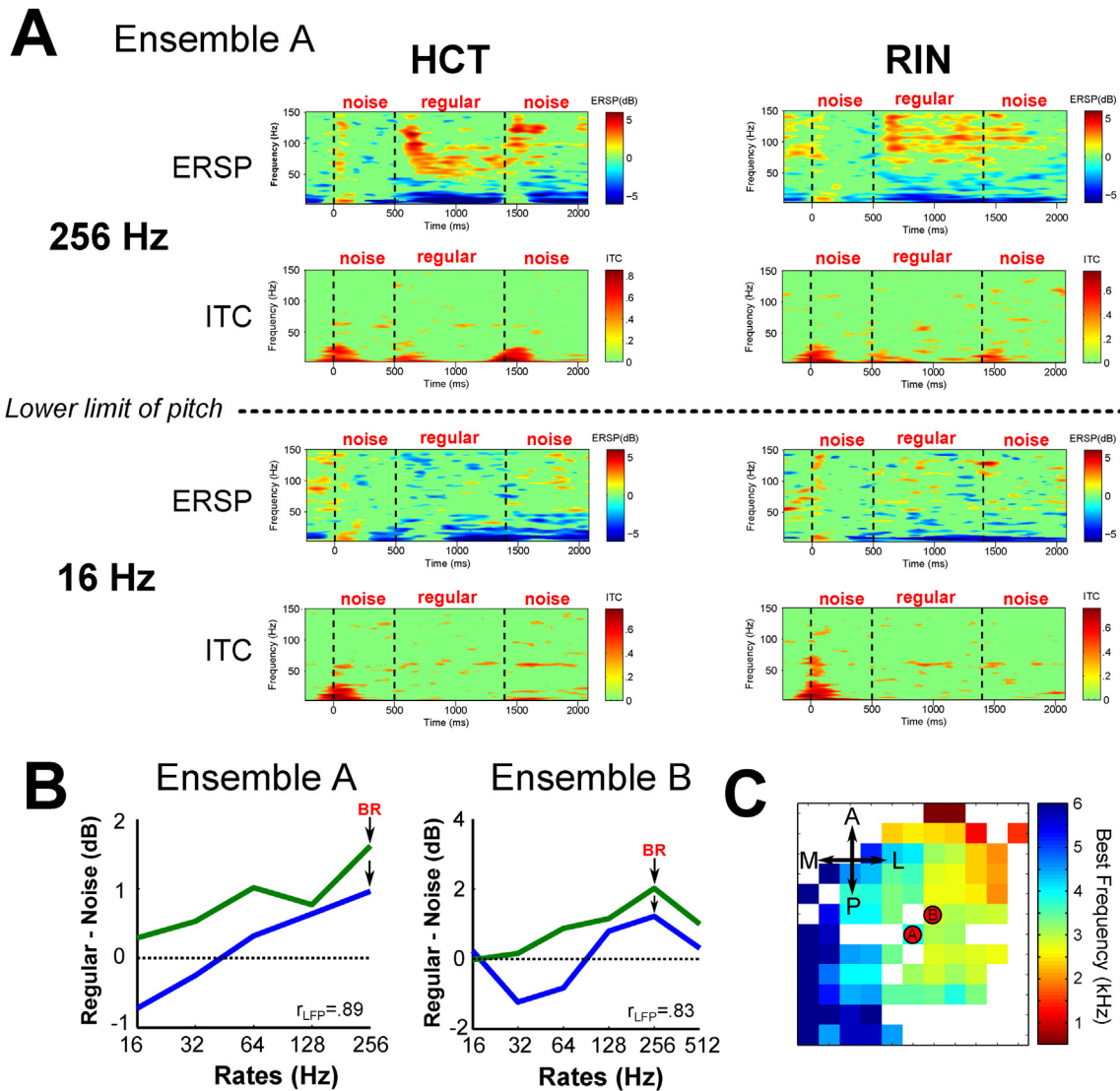


**Fig. 4 – Examples of pitch LFP responses. (A)** Time-frequency decompositions of LFP responses in the monkey auditory cortex. Shown are the event-related spectral perturbation (ERSP) (top panels) and inter-trial phase coherence (ITC) (bottom panels) in response to rates below and above the lower limit of pitch (16 and 256 Hz, respectively) **(B)** Tuning curves of LFP power in the high-gamma frequency range (80–120 Hz) in response to RINs and HCTs at multiple repetition rates (left: the tuning curve for the LFP shown in A, right: tuning curve for another LFP example). The solid green lines show the tuning curve in response to the RIN and the blue solid lines show that in response to HCT. **(C)** Locations of the recording sites for two LFPs showing pitch responses shown in A and B denoted by the red circles ('A' for LFP in the left panel and 'B' for LFP in the right panel in Fig. 4B). The background colour map depicts the tonotopic map based on the averaged BFs of single-unit activity of the right STP of Monkey.

Pitch-related SUA responses were demonstrated in the anterolateral low-frequency part of A1 in a similar area to that reported previously in the marmoset (Bendor & Wang, 2005) (Fig. 5A upper right quadrant of recording area). We also demonstrated LFP pitch-related responses in the same area, and often saw an overlap in responses meeting our criteria in LFP and SUA responses from the same site. However, in the present study both pitch-related single-units and LFPs were also demonstrated in other subdivisions of auditory cortex in both animals (Fig. 5A). The BR of pitch-related SUA and LFP responses corresponded to the BF of the units in certain cases

(Fig. 5B). Responses meeting our criteria did not always follow tuning to sine tone frequencies: only 33% (8/24) of SUA and 23% (6/21) of LFP showed similar tuning ( $\pm 1$  octave) among the responses to RIN, HCT, and sine tones with no significant correlation between the BRs and BFs in both SUA and LFP (SUA:  $\rho = .16$ ,  $p = .47$ , LFP:  $\rho = .24$ ,  $p = .30$ , Spearman correlation, Fig. 5B). The locations of the recordings that showed similar SUA or LFP tuning in response to the three types of stimuli and such correspondences were not unique to anterolateral A1 in low-frequency areas, occurring also in high-frequency tonotopic regions (Figure S5).

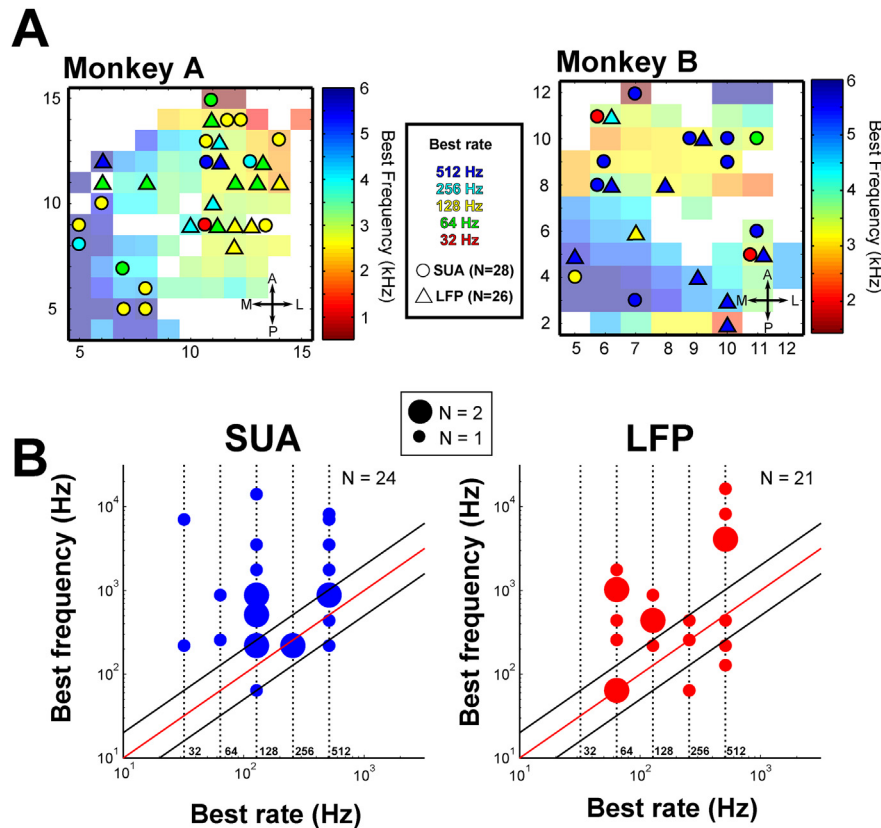


**Fig. 5 – Locations of SUA and LFP pitch responses and the relationships between BRs and BFs (A) Locations of the SUA and LFP showing pitch responses on the supratemporal planes (STP) of the two animals. The circles denote the locations of SUA and the triangles denote the locations of LFP. The colours of the symbols indicate the best rates (BR) of either SUA (circle) or LFP (triangle). The background colour map depicts the tonotopic map based on the averaged best frequencies (BFs) of all the recorded neurons at each pixel (1 mm spacing) from the right STP of two monkeys (Monkey A: N = 142; Monkey B: N = 160), which are partially overlapped with the single-unit data shown in B. (B) BRs and BFs of SUA (left) and LFP (right) pitch responses with no significant correlation (SUA:  $P = .47$ , LFP:  $P = .30$ ). The units which were not tested with sine tones (4 units for SUA, 5 units for LFP) were not included in this analysis (SUA: N = 24; LFP: N = 21). The two circle sizes indicate the number of pitch SUAs (blue circle) or LFPs (red circle). The red line is a unity slope line and represents units with their BF equal to the BR. The black lines denote  $\pm$  one octave from the red line.**

### 3. Discussion

The present work provides a basis for understanding the coding and organisation of pitch-related processing relevant to humans, using both pitch-associated stimuli that are broadband like common communication sounds, and simple sine tones. We are cautious about inferring universal pitch mechanisms applicable to all species, but use a non-human primate model that allows comparison with behaviour and opportunistic neurophysiology from humans, and systematic neurophysiology from ferrets and from non-human primates. Non-human primates, such as the macaque, serve as a model for human pitch perception given their similar sensory frequency ranges and perceptual pitch ranges (Joly et al., 2014; Tomlinson, 1988), and the similar anatomical and physiological organisation of their auditory cortices (Baumann et al., 2013). The use of the macaque model allows us to assess pitch-related responses at the level of single-units (SUA) and ensembles (LFP) using combined criteria for pitch-related responses based both on similar responses to common pitch

and established perceptual limits. The data can be compared to previous studies in marmosets and ferrets, based on SUA or LFPs, and to human studies that assess ensemble activity based on LFPs and blood flow responses.

The data show responses associated with broadband pitch in auditory cortex in the form of SUA and LFPs. Pitch-related SUA and LFPs are sometimes present in the same recording site but not always. The best rate (BR) responses associated with pitch SUA and LFP sites were not correlated with the BF responses of neurons (Fig. 5B) assessed with sine tones. Pitch-related SUA and LFPs were distributed across auditory cortex (Figure S5).

#### 3.1. Putative primate pitch representations at the level of single units and LFPs

Previous primate studies of pitch SUA (Bendor & Wang, 2005) have used as a model the marmoset, in which behavioural pitch processing and auditory neural organisation also show similarities to humans (Song, Osmanski, Guo, & Wang, 2016;

Wang & Walker, 2012). However, we are not aware of any animal work that uses the behavioural pitch range of animals as a criterion to define pitch responses as we do in this study for macaques. With regard to pitch regions, organisation of auditory cortex is similar in the marmoset, the macaque and the human (Wang & Walker, 2012).

Based on our minimum criteria, the present macaque data show responses associated with the pitch of complex sounds in 13% of single units ( $n = 28$ ) and 17% of LFP recording sites ( $n = 26$ ). Marmoset neurophysiology (Bendor & Wang, 2005) reveals responses to three-component missing fundamental stimuli with similarly spaced harmonics (likely associated with a common pitch) in different frequency regions. The responses were demonstrated in 39% of neurons (51/131) in anterolateral A1, where the units were also responsive to sine tones, but less than 3% of all of the recorded neurons showed significant correlations between the responses to pure tones and missing fundamentals (Fig. 3B in their study). In the present study we used criteria for a pitch response based on a requirement for similar responses to two kinds of broadband pitch evoking stimuli in the proven pitch range and found only 8 neurons (4%, 8/210) to show similar tuning to sine tones and broadband pitch stimuli (Figure S5). There was no correlation at the population level ( $N = 24$ , Fig. 5B). Neuronal pitch responses that meet this criterion were observed across auditory cortex without such striking concentration in a small area (Figure S5).

The responses that we have observed to pitch-associated broadband stimuli are parsimoniously explained as pitch responses, but we have considered further tests and other possibilities. We have varied the salience of the pitch by changing pitch value from a region in which it is zero (below the lower limit) to a region in which it is above zero (above the lower limit) but a predicted property of a pitch response would be to increase with salience at fixed pitch value. This could be tested in further experiments by varying salience at fixed pitch values by increasing the number of iterations for the RIN. We note, however, that this modulation of salience was performed in Griffiths et al. (2010) (discussed below), which used similar stimuli, and showed linearly increasing LFP oscillatory response magnitude with higher salience. Other tests might include variation the regularity of click trains to vary the salience as in (Bendor & Wang, 2010; Lu, Liang, & Wang, 2001). However, our experiment uses only two different types of acoustic stimuli with the same pitch, it is possible that other acoustic stimuli with the same pitch might not evoke a response. Also pitch responses based on similar criteria used in this paper are observed throughout the entire auditory cortex in marmosets (Bendor & Wang, 2010), therefore a difference or stricter criteria might contribute to the localisation of the pitch center (Bendor & Wang, 2010) which was not tested here.

Human recording studies have examined responses associated with pitch at the level of LFPs (Griffiths et al., 2010). High gamma responses at the transition from random noise to RIN have been demonstrated in auditory cortex, when the repetition rate is in the range that produces the perception of pitch in humans. The responses were recorded from multi-contact electrodes placed in human core and lateral belt homologues. Data from eight patients confirm the existence of such

responses (Gander et al., 2019) for both core and belt analogues in medial and lateral Heschl's Gyrus (HG) and belt/parabelt homologues of planum temporale and lateral superior temporal gyrus. The responses in humans were widely distributed, which is consistent with recent fMRI findings (Allen, Burton, Olman, & Oxenham, 2017), although there is some clustering of areas in the lateral part of HG in human belt homologues.

We considered the nature of the neural code for pitch in view of our neuronal and ensemble data. Macaques and humans can both discriminate pitch values above 30 Hz for harmonic complexes that differ in pitch by less than a semitone (Joly et al., 2014). Even the most highly tuned responses shown in Figure S1 do not allow pitch encoding with such precision based on the simplest possible coding scheme using the tuned firing rate of single neurons. Alternatively, pitch encoding could be based on coding by groups of neurons (Bizley & Walker, 2010). The LFP data that are recorded here do not provide any direct evidence for or against the representation of pitch value in networks: it is only possible to suggest that the data do not support local organisation of tuning that might produce finer tuning of LFPs than single unit pitch responses. The spatial separation between pitch-related units and pitch-related LFPs in this study suggests that we need to consider pitch encoding systems in which the responses are not ordered either by BF or BR. A computational study of connectivity in human auditory cortex based on LFP pitch data provides support for a system with prominent back projections from belt to core homologues that we have interpreted in terms of a predictive coding account (Kumar et al., 2011).

### 3.2. Localization of primate pitch responses

The previous marmoset neurophysiological study (Bendor & Wang, 2005) shows pitch SUA restricted to the anterolateral part of A1. LFP responses associated with pitch in humans in the form of gamma oscillations (Griffiths et al., 2010) have been demonstrated more widely, in both core and belt homologues. Functional imaging studies in humans, reviewed in (Griffiths & Hall, 2012) have sought an area specialized for pitch coding and a body of evidence supports the existence of pitch specialisation outside of human core homologues (Norman-Haignere et al., 2013). Different studies have found maximal pitch correlates in either lateral HG or planum temporale (PT), largely depending on the type of pitch stimulus used. It should be noted that in the previous work, although a number of these studies show maxima outside of core homologues, significant pitch-related activity is also demonstrated within core homologues (see (Griffiths et al., 2010) for discussion).

In the present study, despite employing stringent criteria for the presence of pitch-related SUA and LFPs, the sites showing activity were found to be distributed across a much wider region of auditory cortex than in the previous marmoset study. There is some clustering of pitch-related responses in this study within anterolateral A1 as in the marmoset, especially in monkey A (Fig. 5A), but without the same degree of specialisation within this small area. The clustering of pitch-related responses is also demonstrated in Figure S4, which

also shows increased correlation between the two types of pitch stimulus in the same small area. Our principal conclusion from this study, however, is that the majority of SUA and LFP pitch-related responses are outside of this area. Work based on SUA in the ferret (Bizley, Walker, Silverman, King, & Schnupp, 2009) also suggests mechanisms for pitch representation that are present in A1 and multiple other auditory cortical areas.

### 3.3. Comparison of pitch responses to complex tones and sine tones

We have considered whether the pitch-related responses to broadband sounds (RIN and HCT) might show best rate (BR) tuning similar to the best frequency (BF) tuning observed with sine tones. In the previous study of the marmoset (Bendor & Wang, 2005), this relationship was examined in 15 units (Fig. 3B in (Bendor & Wang, 2005)), and a correlation was demonstrated for 13 units where the corresponding BRs and BFs were within an octave (although all units examined had an overlapped response). That report described the pitch responsive units as showing similar responses to sine tone frequency and missing fundamental HCTs ‘in general’, although 50 neurons in the pitch region were described as responding only to broadband sounds, with 10 of these demonstrating pitch responses that were tuned to different types of pitch-evoking stimuli and to pure tones. Previous studies have shown that missing fundamental pitch is perceived by the macaque (Tomlinson, 1988). One previous neurophysiological study did not find any single-units that responded to missing fundamental stimuli in parallel to a pure tone at the same fundamental frequency in macaque A1 (Schwarz & Tomlinson, 1990). Another study where macaque calls were presented to macaques (Kikuchi, Horwitz, Mishkin, & Rauschecker, 2014) demonstrated that 3 of 88 units in A1 showed similar pitch responses to the fundamental frequency of the coo stimuli and corresponding sine tones. In the present study, we have examined the responses to sine tones, RINs and HCTs in 210 single units and 149 LFP recording sites. We have found a correspondence between BF and BR tuning (within an octave) in 8 of 24 single units that show pitch-related responses and 6 of 21 LFP sites that show pitch-related responses (Fig. 5). Amongst the other 16 units and 15 sites that produced pitch responses, there were very large differences between the sine tone tuning and the broadband pitch tuning. The pitch-evoking stimuli have the same energy and bandwidth as the noise and noise was preceding all the pitch stimuli therefore, even if noise inhibited the neural response, the pattern of tuning curve should be the same. Units and recording sites demonstrating correspondence between pitch-related and frequency tuning did occur in anterolateral A1, but they also occurred in high frequency cortex (Figure S5).

There have been fMRI studies designed to search for a pitch centre in auditory cortex (e.g., (Hall & Plack, 2009)), in which it is argued that any putative pitch centre should respond in a similar manner to broadband complex sounds and pure tones that produce the same pitch. This is an interesting suggestion, but there are reasons to believe that this is an excessively stringent criterion to place on a system intended for the

perception of the pitch of primate communication sounds (including speech and music in the case of humans). Although the pitch of sine tones can be matched to the pitch of broadband sounds, and both can be ordered from low to high, and both can be used to create sequential patterns, extracting a specific pitch value from broadband sounds requires the co-ordination of neural processing across frequency and over time that is orders of magnitude more complex than detecting an isolated spectral peak. Indeed, the cochlea isolates and orders sine tones along the tonotopic axis before neural processing of the stimulus even begins. So it seems likely that the processing of broadband pitch involves neural assemblies that are not required to identify the pitch of sine tones. More specifically, with regard to neurophysiology, unique responses to both narrowband and broadband sounds are well described and we do not feel the absence of a narrowband response should exclude a unit or LFP measure from consideration as being part of a pitch coding mechanism.

In summary, the present study shows that, in macaques, there is SUA and LFP activity distributed across auditory cortex corresponding to the pitch of broadband sounds. Similar tuning related to pitch and frequency can be demonstrated, but in a minority of recordings. The SUA and LFPs have some tendency to cluster on the edge of A1, but not to the same extent as in previous studies involving the marmoset. The data do not support accounts in which pitch perception of broadband sounds is explained by the activity of single neurons, or activity within a single ‘pitch centre’. A more complex and distributed system is suggested instead involving at least two types of neural activity (spiking and LFP oscillations) and multiple divisions of primary and non-primary auditory cortex.

---

## 4. Materials and Methods

Two adult male Rhesus monkeys (*Macaca mulatta*, weighing 9–13 kg, age 5–8) participated in this study. All animal work and procedures were approved by the UK Home Office and by the Animal Welfare and Ethical Review Body at Newcastle University. The animals from a group housed colony (the pen size ranging from 130 × 240 cm to 215 × 240 cm, width/depth, with 230 cm height) were studied. The work complies with the Animal Scientific Procedures Act (1986) on the care and use of animals in research, and with the European Directive on the protection of animals used in research (2010/63/EU). We support the principles on reporting animal research stated in the consortium on Animal Research Reporting of In Vivo Experiments (ARRIVE). All persons involved with the macaques in this project were Home Office certified and the work was strictly regulated by the U.K. Home Office.

### 4.1. Experimental design and stimuli

The electrophysiological recording sessions were conducted on two to three days per week in a single-walled acoustic chamber installed with foam isolation elements (IAC). The animal sat in a monkey chair with its head fixed, facing a video monitor (24" Samsung, LCD) located .6 m directly in front of it in a darkened room. The animal was trained to

perform a visual fixation task and initiated a trial by fixating a spot for 900 ms and the animals neither attended auditory stimuli nor were engaged in a pitch task which might possibly affect neural representations of pitch in the auditory cortex (Fishman, Reser, Arezzo, & Steinschneider, 1998). Fixating the spot triggered presentation of the sound for that trial (Fig. 1), which consisted of a .5 sec burst of noise, a .9 sec pitch-evoking stimulus (either a regular interval noise [RIN] or a harmonic complex tone [HCT]), and another .9-sec burst of noise. The animal was required to fixate the spot throughout the entire 2.3 sec of sound to receive a reward (juice drop, ~.2 ml), which occurred approximately ~.5 sec after the offset of sound. The sounds were presented free field at ~75 dB SPL binaurally from two speakers positioned approximately 30° to the left and right of the display.

The HCTs were composed of all harmonics of the fundamental, F0, in the region below 4000 Hz. The F0 was 16, 32, 64, 128, 256, or 512 Hz. The harmonics were of equal amplitude and they were added in random phase, which gave the tone a buzzy timbre. For comparison, the musical note A above middle C on the piano keyboard has a pitch value of 440 Hz. The RINs were created from a broadband noise using a delay-and-add procedure with 16 iterations, which gave the RIN a strong pitch at the reciprocal of the delay (Patterson et al., 1996). Three exemplars were created for each stimulus condition. The delays were set to produce pitch values of 16, 32, 64, 128, 256, and 512 Hz to match those of the HCTs. The RINs have the same energy and bandwidth as the noise, and there are similar fluctuations in their temporal envelopes, so neurons that simply respond to the onset of broadband sounds or their spectro-temporal envelopes will produce similar responses to all of them (S6). All the stimuli (noise, RIN, and HCT) were pass-band filtered between 4 and 4000 Hz and a pink filter was applied. Neurons involved in analysing the temporal fine structure of the sounds would be expected to increase their firing rate at the onset of the RIN, despite the fact that there is no change in stimulus energy or in the short term statistics of the spectro-temporal envelope. 28 LFPs and 36 SUAs were recorded in the session using the rates up to 256 Hz and 55 LFPs and 84 SUAs using the rates up to 512 Hz in Monkey A. In Monkey B, all 66 LFPs and 90 SUAs were recorded in the sessions using the rates up to 512 Hz. All stimuli were scaled to the same root-mean-square (RMS) value. The stimuli were generated with 16-bit resolution at a sampling rate of 44.1 kHz using MATLAB 7.10 (MathWorks Inc.).

#### 4.2. Electrophysiological recordings

MRI was used for chamber placement and electrode guidance. The MRI structural and functional data were obtained with a 4.7T scanner (Bruker BioSpin, Etlingen, Germany). A customized MRI compatible head post and cylindrical recording chamber (19 mm diameter, PEEK) were implanted under general anesthesia. The recording chamber was positioned stereotactically over the right hemispheres of both animals to target the auditory cortex where tonotopic organization was observed using fMRI (Petkov, Kayser, Augath, & Logothetis, 2006; Tanji et al., 2010). The locations of the chambers were confirmed physiologically using tonotopic topography of single-unit activity (SUA); in both cases it was found to cover

the caudal core (including field A1) and the lateral belt of auditory cortex (Figs. 2C and 3C). Up to three independently driven tungsten microelectrodes (.1–1.0 M $\Omega$ , epoxyite insulation, FHC, Bowdoin, ME) were inserted through guide tubes and lowered into the auditory cortex based on the post-operative MRI. Each electrode was independently advanced using a remote-controlled 4-channel microstep-multidrive system (NAN-SYS-4, Plexon, Inc., Dallas, TX). We aimed to locate auditory neurons using search stimuli with various sounds (e.g., noise, tones, complex natural sounds), however, we did not attempt to select neurons based on their stimulus preference nor the shape of their spiking activity. The signal from each electrode was passed through a head stage with gain one and high input impedance (HST/8050-G1, Plexon Inc.) and then split to extract the spiking activity and the local field potentials through a preamplifier system (PBX2/16sp/16fp, Plexon Inc.). The spike signals were filtered with a pass-band between 150 and 8,000 Hz, further amplified, and then digitized at 40 kHz. The LFP signals were also pass-band filtered between .7 and 500 Hz, amplified, and digitized at 1 kHz. Voltage-thresholding was applied to spiking activity during electrophysiological recordings and a template-matching Principal Component Analysis (PCA) was applied offline to isolate single neurons.

Time stamps indicating the timing of auditory stimulus, behavioural response, and reward events were sent through a Windows CORTEX (Salk Institute) dual computer system, and continuous data, such as sound waveforms and eye movements monitored by an infrared-based eye-tracking system, were sent to a Multichannel Acquisition Processor system (MAP, Plexon, Inc.) and then integrated with the spike and LFP data. During the recording session, spikes were initially sorted online by real-time acquisition programs using template matching and PCA clustering methods (RASPUTIN, Plexon). Estimation of the frequency-tuning profiles of the neurons were examined online (Neuroexplorer, Nex Technologies, MA). Throughout the recording sessions, we monitored neuronal activity visually with an oscilloscope (HM407-2, HAMEG) and aurally through headphones (HD 280 Professional, Sennheiser). Pre-processing and data analysis were performed on MATLAB.

#### 4.3. LFP analysis

For LFPs, the 50 Hz electrical line noise was removed and locally detrended using a 1-sec window with .5 sec steps with Chronux MATLAB scripts (<http://chronux.org>). A time bandwidth product of five and nine Slepian taper functions was used. To evaluate the average temporal change in the spectral power and phase-consistency of the LFP, event-related spectral perturbation (ERSP) and inter-trial phase coherence (ITC) were calculated for frequencies between 2.5 and 150 Hz using a 3-cycle Morlet wavelet at the lowest frequency linearly increasing the number of cycles for higher frequencies. The ERSP was measured with a sliding window (700 ms) and averaged across trials. The consistency of phase angles across trials (i.e., ITC) was calculated by the length of the average population vector of unit-length vectors from each trial. The length of the average vector reflects the proximity of vectors across trials. An ITC value of 0 indicates a uniform distribution

of phase angles across trials. This time-frequency decomposition was made using a modified EEGLAB MATLAB script (Delorme & Makeig, 2004). Baseline power normalization at each frequency was performed during a baseline period of 500 ms prior to the regular stimulus onset. The data were first averaged across trials and decibel-normalized. Significance levels were evaluated by randomly shuffling the spectral estimates from different time windows during the 500 ms baseline period (i.e., the period of first noise presentation,  $p < .05$ , bootstrap significance level). Auditory LFPs were defined as a significant increase in ERSP in the high-gamma range between 80 and 120 Hz during the 2300 ms sound presentation period compared to the baseline activity 500 ms prior to sound onset using a two-sample t-test ( $p < .01$ ).

#### 4.4. Spike analysis

The spike density function was created to construct spike density peri-stimulus time histograms (PSTHs). This involved convolving spike counts with an anti-causal exponential function (time constant for the growth phase = 1 ms, decay phase = 20 ms) (Thompson, Hanes, Bichot, & Schall, 1996). This asymmetric procedure avoids the influence of spiking activity during the pre-stimulus period, as would result from a symmetric kernel (e.g., Gaussian kernel), and improves temporal precision by measuring more accurate response latencies. The PSTH was normalized to the average variability (SD) of the smoothed baseline firing rates across all the baseline activity during a pre-stimulus period. Auditory neurons were defined as neurons that elicited a significant increase in activity for three consecutive 1-ms bins, that is, activity 2.0 SD above the baseline activity during the 500 ms baseline prior to sound onset across ~20 trials. We defined a neuron as “auditory responsive” if at least one of the stimuli elicited an excitation response throughout the stimulus presentation period (2300 ms).

#### 4.5. Tuning curve

To construct turning curves in response to RIN and HCT stimuli, mean baseline-corrected power estimates in the high-gamma range (80–120 Hz) and mean firing rates were extracted for LFPs and SUAs, respectively, during the entire regular sound presentation period (501–1400 ms after sound onset) across trials in response to each stimulus. We then subtracted the mean response magnitude during the noise interval prior to a regular stimulus (1–500 ms after sound onset). The Spearman correlation (nonparametric rank correlation) was used for the calculations of correlation coefficients between tuning curves for RIN and HCT.

#### 4.6. Tonotopic map

To construct a tonotopic map for each animal, normalized mean firing rates were calculated after the subtraction of the average baseline firing rate 300 ms prior to sound onset across all the sine tone stimuli. For auditory neurons with significant increases in their firing rates ( $>3SD$ ) during the sound presentation period, tuning curves were constructed using a peak

response magnitude (i.e., maximum response firing rate during the sound presentation period). The threshold of significance was different from that used for the main experiment (i.e.,  $> 2SD$ ) to obtain the clear tonotopic map. The frequency that elicited the maximum response on the tuning curve function was defined as the best frequency (BF) for the neuron. In separate recording blocks, 7 sine tones ranging from 220 to 14080 kHz in octave steps or 10 sine tones ranging from 32 to 16384 Hz in octave steps were randomly presented to determine the neuron's best frequency (BF). The colour map was created based on the averaged best frequencies (BF) of auditory neurons recorded from each grid (1 mm spacing) and smoothed by a moving-average of 3 mm by 3 mm for display purposes. Testing with sine tones was not always performed along with the main experiment using RIN and HCT due to animal behavioural states and stability of neuronal data.

The number of independent samples from each animal and all the criteria used to select neuronal responses to support the findings are based on the criteria described above and all the results in this report are based on offline analysis.

---

#### Conflict of interest statement

The authors have no conflicts of interest.

---

#### Data availability

The data used to generate the results and figures underlying the findings are publicly available on the Open Science Framework at <https://osf.io/arqp8/>. No part of the study procedures was pre-registered prior to the research being conducted.

---

#### Open Practices

The study in this article earned Open Materials and Open badges for transparent practices. Materials and data for the study are available at <https://osf.io/arqp8/>.

---

#### CRediT authorship contribution statement

**Yukiko Kikuchi:** Data curation, Formal analysis, Investigation, Methodology, Validation, Visualization, Writing - original draft. **Sukhbinder Kumar:** Methodology, Validation, Visualization, Writing - review & editing. **Simon Baumann:** Data curation, Formal analysis, Investigation, Validation, Visualization, Writing - review & editing. **Tobias Overath:** Methodology, Validation, Writing - review & editing. **Phillip E. Gander:** Methodology, Writing - review & editing. **William Sedley:** Methodology, Validation, Writing - review & editing. **Roy D. Patterson:** Conceptualization, Methodology, Writing - original draft. **Christopher I. Petkov:** Funding acquisition, Investigation, Methodology, Project administration, Resources, Supervision, Validation, Writing - review & editing. **Timothy D. Griffiths:** Conceptualization, Funding acquisition,

Investigation, Project administration, Resources, Supervision, Validation, Writing - original draft.

## Acknowledgements

This work was supported by Wellcome Trust [TDG, WT091681MA; CIP, Investigator Award WT092606AIA]; and BBSRC [CIP joint with Quoc Vuong, BB/J009849/1]. We thank O. Joly for useful discussions and D. Hunter and A. Thiele for providing assistance or materials. We also thank the reviewer D. Bendor for constructive comments on the manuscript.

## Supplementary data

Supplementary data to this article can be found online at <https://doi.org/10.1016/j.cortex.2019.07.005>.

## REFERENCES

- Allen, E. J., Burton, P. C., Olman, C. A., & Oxenham, A. J. (2017). Representations of pitch and timbre variation in human auditory cortex. *Journal of Neuroscience*, 37, 1284–1293.
- Baumann, S., Petkov, C. I., & Griffiths, T. D. (2013). A unified framework for the organization of the primate auditory cortex. *Frontiers in Systems Neuroscience*, 7, 11.
- Bendor, D., & Wang, X. (2005). The neuronal representation of pitch in primate auditory cortex. *Nature*, 436, 1161–1165.
- Bendor, D., & Wang, X. (2010). Neural coding of periodicity in marmoset auditory cortex. *Journal of Neurophysiology*, 103, 1809–1822.
- Bizley, J. K., & Walker, K. M. M. (2010). Sensitivity and selectivity of neurons in auditory cortex to the pitch, timbre, and location of sounds. *The Neuroscientist*, 16, 453–469.
- Bizley, J. K., Walker, K. M. M., Nodal, F. R., King, A. J., & Schnupp, J. W. H. (2013). Auditory cortex represents both pitch judgments and the corresponding acoustic cues. *Current Biology*, 23, 620–625.
- Bizley, J. K., Walker, K. M. M., Silverman, B. W., King, A. J., & Schnupp, J. W. H. (2009). Interdependent encoding of pitch, timbre, and spatial location in auditory cortex. *Journal of Neuroscience*, 29, 2064–2075.
- Delorme, A., & Makeig, S. (2004). EEGLAB: An open source toolbox for analysis of single-trial EEG dynamics including independent component analysis. *Journal of Neuroscience Methods*, 134, 9–21.
- Fishman, Y. I., Reser, D. H., Arezzo, J. C., & Steinschneider, M. (1998). Pitch vs. spectral encoding of harmonic complex tones in primary auditory cortex of the awake monkey. *Brain research*, 786, 18–30.
- Gander, P. E., Kumar, S., Sedley, W., Nourski, K. V., Oya, H., Kovach, C. K., et al. (2019). Direct electrophysiological mapping of human pitch-related processing in auditory cortex. *Neuroimage* (in press).
- Ghazanfar, A. A., Turesson, H. K., Maier, J. X., van Dinther, R., Patterson, R. D., & Logothetis, N. K. (2007). Vocal-tract resonances as indexical cues in rhesus monkeys. *Current Biology*, 17, 425–430.
- Griffiths, T. D., & Hall, D. A. (2012). Mapping pitch representation in neural ensembles with fMRI. *Journal of Neuroscience*, 32, 13343–13347.
- Griffiths, T. D., Kumar, S., Sedley, W., Nourski, K. V., Kawasaki, H., Oya, H., et al. (2010). Direct recordings of pitch responses from human auditory cortex. *Current Biology*, 20, 1128–1132.
- Hackett, T. A. (2011). Information flow in the auditory cortical network. *Hearing Research*, 271, 133–146.
- Hall, D. A., & Plack, C. J. (2009). Pitch processing sites in the human auditory brain. *Cerebral Cortex*, 19, 576–585.
- Ives, D. T., & Patterson, R. D. (2008). Pitch strength decreases as F0 and harmonic resolution increase in complex tones composed exclusively of high harmonics. *The Journal of the Acoustical Society of America*, 123, 2670–2679.
- Joly, O., Baumann, S., Poirier, C., Patterson, R. D., Thiele, A., & Griffiths, T. D. (2014). A perceptual pitch boundary in a non-human primate. *Perception Science*, 5, 998.
- Kikuchi, Y., Horwitz, B., Mishkin, M., & Rauschecker, J. P. (2014). Processing of harmonics in the lateral belt of macaque auditory cortex. *Auditory Cognitive Neuroscience*, 8, 204.
- Krumbholz, K., Patterson, R. D., Seither-Preisler, A., Lammertmann, C., & Lütkenhöner, B. (2003). Neuromagnetic evidence for a pitch processing center in Heschl's Gyrus. *Cerebral Cortex*, 13, 765–772.
- Kumar, S., Sedley, W., Nourski, K. V., Kawasaki, H., Oya, H., Patterson, R. D., et al. (2011). Predictive coding and pitch processing in the auditory cortex. *Journal of cognitive neuroscience*, 23.
- Logothetis, N. K., Pauls, J., Augath, M., Trinath, T., & Oeltermann, A. (2001). Neurophysiological investigation of the basis of the fMRI signal. *Nature*, 412, 150–157.
- Lu, T., Liang, L., & Wang, X. (2001). Temporal and rate representations of time-varying signals in the auditory cortex of awake primates. *Nature Neuroscience*, 4(11), 1131–1138.
- Mukamel, R., Gelbard, H., Arieli, A., Hasson, U., Fried, I., & Malach, R. (2005). Coupling between neuronal firing, field potentials, and fMRI in human auditory cortex. *Science*, 309, 951–954.
- Norman-Haignere, S., Kanwisher, N., & McDermott, J. H. (2013). Cortical pitch regions in humans respond primarily to resolved harmonics and are located in specific tonotopic regions of anterior auditory cortex. *Journal of Neuroscience*, 33, 19451–19469.
- Patterson, R. D., Handel, S., Yost, W. A., & Datta, A. J. (1996). The relative strength of the tone and noise components in iterated rippled noise. *The Journal of the Acoustical Society of America*, 100, 3286–3294.
- Patterson, R. D., Uppenkamp, S., Johnsrude, I. S., & Griffiths, T. D. (2002). The processing of temporal pitch and melody information in auditory cortex. *Neuron*, 36, 767–776.
- Penagos, H., Melcher, J. R., & Oxenham, A. J. (2004). A neural representation of pitch salience in nonprimary human auditory cortex revealed with functional magnetic resonance imaging. *The Journal of Neuroscience*, 24, 6810–6815.
- Petkov, C. I., Kayser, C., Augath, M., & Logothetis, N. K. (2006). Functional imaging reveals numerous fields in the monkey auditory cortex. *PLoS Biology*, 4, e215.
- Pressnitzer, D., Patterson, R. D., & Krumbholz, K. (2001). The lower limit of melodic pitch. *The Journal of the Acoustical Society of America*, 109, 2074.
- Schwarz, D. W., & Tomlinson, R. W. (1990). Spectral response patterns of auditory cortex neurons to harmonic complex

- tones in alert monkey (*Macaca mulatta*). *Journal of Neurophysiology*, 64, 282–298.
- Song, X., Osmanski, M. S., Guo, Y., & Wang, X. (2016). Complex pitch perception mechanisms are shared by humans and a New World monkey. *Proceedings of the National Academy of Sciences of the United States of America*, 113, 781–786.
- Tanji, K., Leopold, D. A., Ye, F. Q., Zhu, C., Malloy, M., Saunders, R. C., et al. (2010). Effect of sound intensity on tonotopic fMRI maps in the unanesthetized monkey. *NeuroImage*, 49, 150–157.
- Thompson, K. G., Hanes, D. P., Bichot, N. P., & Schall, J. D. (1996). Perceptual and motor processing stages identified in the activity of macaque frontal eye field neurons during visual search. *Journal of Neurophysiology*, 76, 4040–4055.
- Tomlinson, R. W. W. (1988). Perception of the missing fundamental in nonhuman primates. *The Journal of the Acoustical Society of America*, 84, 560–565.
- Walker, K. M. M., Bizley, J. K., King, A. J., & Schnupp, J. W. H. (2011). Cortical encoding of pitch: Recent results and open questions. *Hearing Research*, 271, 74–87.
- Wang, X., & Walker, K. M. M. (2012). Neural mechanisms for the abstraction and use of pitch information in auditory cortex. *Journal of Neuroscience*, 32, 13339–13342.